

## Research



**Cite this article:** Büscher TH, Kryuchkov M, Katanaev VL, Gorb SN. 2018 Versatility of Turing patterns potentiates rapid evolution in tarsal attachment microstructures of stick and leaf insects (Phasmatodea). *J. R. Soc. Interface* **15**: 20180281.  
<http://dx.doi.org/10.1098/rsif.2018.0281>

Received: 24 April 2018

Accepted: 30 May 2018

### Subject Category:

Life Sciences – Mathematics interface

### Subject Areas:

evolution, biomechanics, environmental science

### Keywords:

attachment, adhesion, cuticle, surface, functional morphology, Turing patterns

### Author for correspondence:

Thies H. Büscher

e-mail: [tbuescher@zoologie.uni-kiel.de](mailto:tbuescher@zoologie.uni-kiel.de)

Electronic supplementary material is available online at <https://dx.doi.org/10.6084/m9.figshare.c.4125029>.

# Versatility of Turing patterns potentiates rapid evolution in tarsal attachment microstructures of stick and leaf insects (Phasmatodea)

Thies H. Büscher<sup>1</sup>, Mikhail Kryuchkov<sup>2</sup>, Vladimir L. Katanaev<sup>2,3</sup> and Stanislav N. Gorb<sup>1</sup>

<sup>1</sup>Department of Functional Morphology and Biomechanics, Zoological Institute, Kiel University, Kiel, Germany

<sup>2</sup>Department of Pharmacology and Toxicology, Faculty of Biology and Medicine, University of Lausanne, Lausanne, Switzerland

<sup>3</sup>School of Biomedicine, Far Eastern Federal University, Vladivostok, Russia

THB, 0000-0003-0639-4699; VLK, 0000-0002-7909-5617; SNG, 0000-0001-9712-7953

In its evolution, the diverse group of stick and leaf insects (Phasmatodea) has undergone a rapid radiation. These insects evolved specialized structures to adhere to different surfaces typical for their specific ecological environments. The cuticle of their tarsal attachment pads (euplantulae) is known to possess a high diversity of attachment microstructures (AMS) which are suggested to reflect ecological specializations of different groups within phasmids. However, the origin of these microstructures and their developmental background remain largely unknown. Here, based on the detailed scanning electron microscopy study of pad surfaces, we present a theoretical approach to mathematically model an outstanding diversity of phasmid AMS using the reaction–diffusion model by Alan Turing. In general, this model explains pattern formation in nature. For the first time, we were able to identify eight principal patterns and simulate the transitions among these. In addition, intermediate transitional patterns were predicted by the model. The ease of transformation suggests a high adaptability of the microstructures that might explain the rapid evolution of pad characters. We additionally discuss the functional morphology of the different microstructures and their assumed advantages in the context of the ecological background of species.

## 1. Background

Stick and leaf insects (Phasmatodea) are a diverse lineage of phytophagous insects exhibiting distinct forms of masquerade imitating leaves or twigs [1]. These insects inhabit a wide distributional range, although their mobility is rather restricted, and underwent rapid radiation during the Cretaceous [2]. This resulted in a high degree of convergent trends due to the realization of specific ecological niches among different local distributions [2–4].

Attachment in insects is generally achieved by maximization of the actual contact area between the attachment structure and the substrate. In phasmids, this is achieved by two types of attachment pads, arolia and euplantulae [5–10], which consist of soft cuticle layers and adapt to the surface profile [11] and thus increase adhesion and friction [12,13]. The arolium, located on the pretarsus, is reported to generate adhesion when activated by pulling from the surface [14]. The euplantulae on each of the four proximal tarsomeres, by contrast, mainly generate friction [14–16]. Depending on the surface structure, however, the contribution of friction and adhesion is different for specific types of surface microstructures [15]. The surface of the arolium is smooth in Euphasmatodea and covered by nubby outgrowths in *Timema*, the sister group of the remaining phasmatodeans [5–7,10,17]. Euplantulae (four to five per leg) possess a variety of attachment microstructures (AMS) in Phasmatodea, with one lineage (*Dinophasma*

**Table 1.** Parameters for the mathematical modelling of figure 1.

| no. | <i>aa</i> | <i>ba</i> | <i>ca</i> | <i>da</i> | <i>diff_a</i> | <i>ab</i> | <i>bb</i> | <i>cb</i> | <i>db</i> | <i>diff_b</i> | <i>F<sub>max</sub></i> | <i>G<sub>max</sub></i> |
|-----|-----------|-----------|-----------|-----------|---------------|-----------|-----------|-----------|-----------|---------------|------------------------|------------------------|
| e   | 0.07      | −0.13     | 0.03      | 0.03      | 0.14          | 0.23      | 0.01      | −0.1      | 0.08      | 3.7           | 0.2                    | 0.5                    |
| f   | 0.079     | −0.08     |           |           |               |           |           |           |           |               |                        |                        |
| g   | 0.11      | −0.06     |           |           |               |           |           |           |           |               |                        |                        |
| h   | 0.11      | −0.17     |           |           |               |           |           |           |           |               |                        |                        |
| m   | 0.14      | −0.10     |           |           |               |           |           |           |           |               |                        |                        |
| n   | 0.23      | −0.16     |           |           |               |           |           |           |           |               |                        |                        |
| o   | 0.099     | −0.16     |           |           |               |           |           |           |           |               |                        |                        |
| P   | 0.3225    | −0.23     |           |           |               |           |           |           |           |               |                        |                        |

(Aschiphasmatinae)) standing out from the others and bearing large adhesive setae [17]. These microscopic structures consist of cuticular protuberances (probably microtrichia according to Richards & Richards [18]) and resemble a set of patterns similar to those observed in insects' corneal patterns [19–21].

The formation of numerous types of patterns in nature can be explained by Alan Turing's reaction–diffusion model [22]. Using this mathematical model, it is possible to explain pattern formation for structures with typical dimensions from 100 nm onwards, such as corneal nanocoatings of insects. Almost the entire variety of corneal nanocoatings was previously modelled by a slight change in both properties and amounts of the reacting elements [19,20]. This mathematical simulation reflects only the formation of a structure's patterns and the size of the cross section of its elements, but is in no way able to predict their height. Perhaps, the height of these structures is influenced by the organization of the underlying layers of chitin and chitosan [23]. The transition from one structure to another can be also detected within a short evolutionary period [24], or in different ommatidia of one insect [25,26], as well as on the corneal lens of one ommatidium, like on Tipulidae eyes [19].

Various phylogenetic [5–7,10,17,27], biomechanic [15] and taxonomic [28–31] studies investigated the diversity of euplantular AMS in Phasmatodea. The AMS provide certain biomechanic properties that influence attachment performance and their specificity to substrates [14–16,32,33]. Most probably various AMS are adapted to different substrates or substrate families within typical ecological niches [17,27,34]. As the rapid radiation of Phasmatodea results in a very local set-up of the ecotypes, similar AMS are found frequently in morphologically similar, but phylogenetic unrelated lineages [17,27]. The high degree of independent origins or reversals of the same type of AMS suggests high adaptability of AMS during the phasmatodean evolution [27]. Therefore, we approached the formation of the different patterns which are present in the AMS of phasmids and evaluated their potential to transformations.

## 2. Material and methods

### 2.1. Animals

Specimens were obtained from various sources either alive, fixed in 70% ethanol or dried. All samples were processed following the procedures previously used [10,17,27]. In the case of dried insects, the cuticle of attachment pads was softened using the procedure described in [35].

### 2.2. Scanning electron microscopy

Fixed samples were dried in an ascending alcohol series and critical-point dried. The dried samples were then sputter-coated with a 15 nm thick layer of gold–palladium. Specimens were examined under the scanning electron microscope (SEM) Hitachi S4800 (Hitachi High-Technologies Corp., Tokyo, Japan) at 5 kV of acceleration voltage.

### 2.3. Modelling

For the model simulation, the software 'Ready' (a cross-platform implementation of various reaction–diffusion systems (<https://github.com/GollyGang/ready>)) was used with the parameters illustrated in tables 1 and 2.

Formula:

$$\begin{aligned} \text{delta}_a &= \max(0, \min(aa^*a + ba^*b + ca, F_{\max})) \\ &\quad - da^*a + \text{diff}_a^* \text{laplacian}_a + d; \\ \text{delta}_b &= \max(0, \min(ab^*a + bb^*b + cb, G_{\max})) \\ &\quad - db^*b + \text{diff}_b^* \text{laplacian}_b; \\ c &= a + b; \\ d &= \text{fmod}(d + \text{laplacian}_d, 0.2). \end{aligned}$$

The first two equations were successfully used in former studies [20]. The third is used for visualization. The last equation is necessary to create an initial noise—a slight uneven distribution of the reagents.

## 3. Results

### 3.1. Attachment microstructures

The evaluation of the euplantular AMS of stick insects revealed eight types of patterns (figure 1): (i) smooth, (ii) undulating, (iii) plateaus, (iv) small nubs, (v) big nubs, (vi) flat pads, (vii) mazes and (viii) ridges (see electronic supplementary material, S1 for descriptions of observed AMS). Furthermore, various transitions between different patterns were observed when re-evaluating the AMS in consideration of the simulated patterns. Certain species possess intermediate types of AMS between the ones described here and are considered to represent evolutionary transient forms of the patterns. In all species, the structures cover the whole euplantula. The AMS were examined at magnifications of 30 000 and 50 000 times to prove the presence of an additional level of nanostructures. Besides the diversity of the illustrated microstructures, no further hierarchical structures were observed (see electronic supplementary material, S2 for high magnification micrographs of representative AMS).

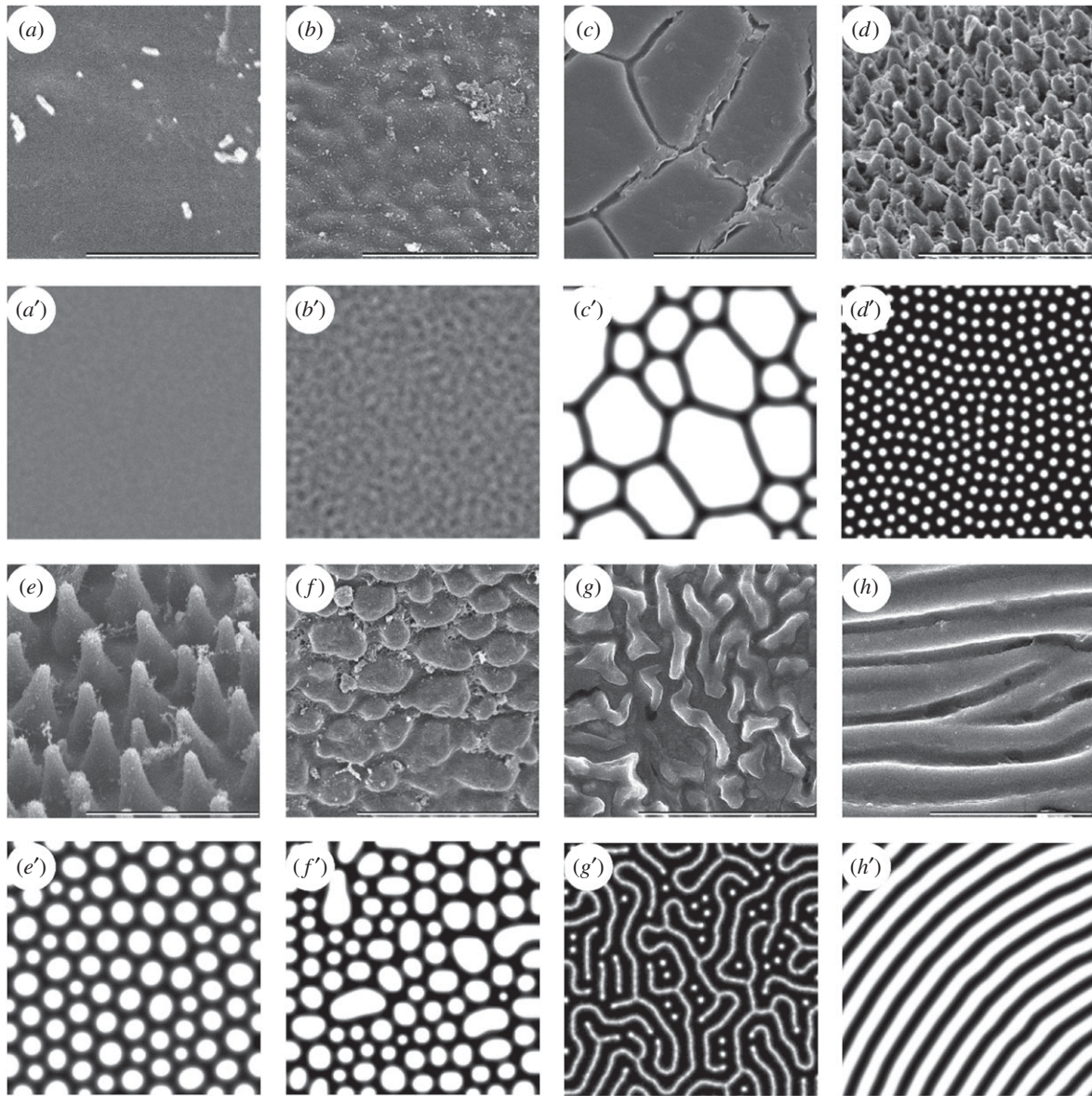


**Figure 1.** The diversity of AMS in Phasmatodea ( $a-h$ ) and the corresponding mathematically modelled Turing patterns ( $a'-h'$ ). ( $a,a'$ ) Smooth type, *Orthomeria pandora* (Aschiphasmatinae). ( $b,b'$ ) Undulating type, *Kalocorinnis wegneri* (Korrinninae). ( $c,c'$ ) Maze type, *Leosthenes aquatilis* (Xeroderinae). ( $d,d'$ ) Small nubs, *Mearnsiana bullosa* (Obriminae). ( $e,e'$ ) Big nubs, *Hemiplasta falcata* (Necrosiinae). ( $f,f'$ ) Flat pad type, *Necrosia annulipes* (Necrosiinae). ( $g,g'$ ) Ridges, *Argosarchus horridus* (Phasmatinae). ( $h,h'$ ) Plateau type, *Epidares nolimetangere* (Dataminae). Scale bars: ( $a-h$ )  $5\ \mu\text{m}$ . Size of simulated area ( $a'-h'$ )  $256 \times 256$  px.

**Table 2.** Parameters for the mathematical modelling of figure 2.

| no. | $aa$   | $ba$  | $ca$ | $da$ | $\text{diff}_a$ | $ab$ | $bb$ | $cb$ | $db$ | $\text{diff}_b$ | $F_{\text{max}}$ | $G_{\text{max}}$ |
|-----|--------|-------|------|------|-----------------|------|------|------|------|-----------------|------------------|------------------|
| a   | 0.09   | -0.14 | 0.03 | 0.03 | 0.14            | 0.23 | 0.01 | -0.1 | 0.08 | 3.7             | 0.2              | 0.5              |
| b   | 0.099  | -0.16 |      |      |                 |      |      |      |      |                 |                  |                  |
| c   | 0.12   | -0.15 |      |      |                 |      |      |      |      |                 |                  |                  |
| d   | 0.17   | -0.15 |      |      |                 |      |      |      |      |                 |                  |                  |
| e   | 0.21   | -0.14 |      |      |                 |      |      |      |      |                 |                  |                  |
| f   | 0.27   | -0.21 |      |      |                 |      |      |      |      |                 |                  |                  |
| g   | 0.3225 | -0.23 |      |      |                 |      |      |      |      |                 |                  |                  |
| h   | 0.32   | -0.21 |      |      |                 |      |      |      |      |                 |                  |                  |
| i   | 0.17   | 0.10  |      |      |                 |      |      |      |      |                 |                  |                  |

### 3.2. Mathematical simulation of attachment microstructures

For modelling purposes, we were able to choose the conditions under which we observed all the types of patterns described

above within the limited area of a two-dimensional section of a potential 12-dimensional array. This means that only two parameters are variables, when the other 10 are constant. Two axes on this graph show interactions between reagents:  $ba$ —the level of inhibition of the chemical  $a$  by the chemical  $b$  and  $aa$ —the

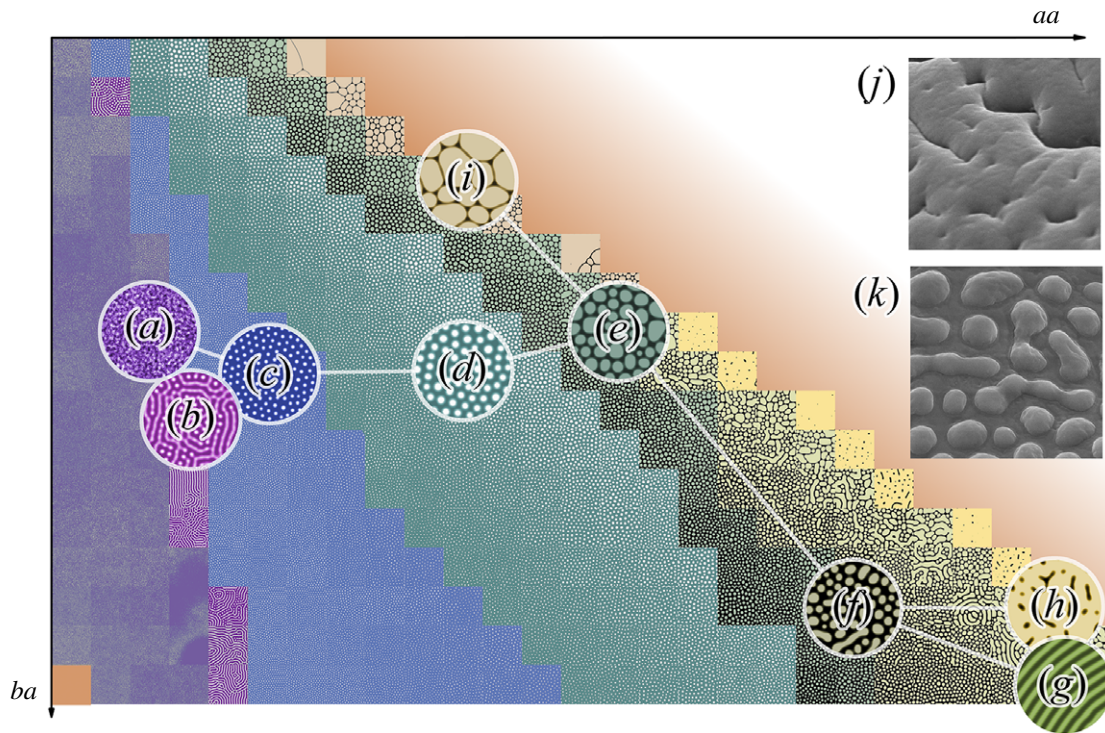


**Figure 2.** Graph showing the examples of patterns in  $aa$  and  $ba$  coordinate space, overlaid with network, nodes ( $a-i$ ) depicting different types of structures, edges showing the most possible ways of transitions between them. ( $a$ ) Undulating type, ( $b$ ) maze type, ( $c$ ) small nubs, ( $d$ ) big nubs, ( $e$ ) flat pad type, ( $f,k$ ) the transition between flat pad and big maze types, and its corresponding AMS (*A. lyratus*), ( $g$ ) ridges, ( $h,j$ ) dimpled pattern and its corresponding AMS (*E. goliath*) and ( $i$ ) plateau type. Horizontal dimensions of images: ( $j,k$ ) are  $5\ \mu\text{m}$ .

self-activation of the component  $a$  (figure 2). The two-dimensional patterns show the concentrations of the reagents, but they do not explain the future formation of three-dimensional structures. We have identified the following types of patterns on this two-dimensional surface. First, the ‘smooth’ type corresponds to the absence of any patterns (figure 1*a'*); probably the most common type, which rarely includes islets of pattern formation. The undulating type (figure 1*b'*, 2*a*) represents unstable predecessors of the stable patterns that are unable to hold the form for a long time and to influence their environment, are prone to large-scale oscillations in the transitional part of the graph. When this type of patterns is stabilized, it can spontaneously pass into maze-type patterns (figure 1*g'*, 2*b*) that, with an increase of the parameter  $aa$ , are quickly transformed into very stable small nubs (figure 1*d'*, 2*c*). The difference between small and big nubs (figure 1*e'*, 2*d*) is not only in size, but also in their types of interaction. With an excessive density, small nubs merge together, while big nubs start to suppress each other: this leads to a decrease in the size of smaller nubs and often to their disappearance. That is why among the big nubs there is a small variety of existing sizes. These two types of patterns are mostly uniform in size and together occupy the largest area of the section of parameters under investigation. With a further increase in the  $aa$  parameter, the loss of the rounded shape of the structures was observed, and we called such a pattern ‘flat pads’ (figure 1*f'*, 2*e*). With a larger  $ba$  parameter, these structures grow evenly in all directions, while with a smaller one, they tend to form oblong structures. In turn, these patterns are transformed into a new type of big maze-like pattern (figure 2*f*), similar to the maze-type pattern, but much larger ones that are also prone to form parallel ridges (figure 1*h'*, 2*g*). Under the condition of the increased  $aa$  parameter, the big maze type of patterns is transformed to the last stable type of patterns—the dimpled

pattern (figure 2*h*). At the top of the graph, flat pad-type structures pass into quasi-stable giant structures separated by thin partitions—the plateau-type pattern (figure 1*c'*, 2*i*). They do not have any internal size limitation.

## 4. Discussion

### 4.1. Functions of attachment microstructures

Especially at elevations or in the canopy, insect attachment needs to be secure in order to avoid animals dropping down and suffering damage. The attachment is also important in the case of landing on the legs after flight or jumping [36]. The high diversity of euplantular AMS suggests their different functions in attachment of Phasmatoidea. Although the functional significance of only a few of the AMS have been addressed through experiments so far [14–16], working principles of some surface patterns can be inferred from studies carried out on representatives of other taxa (e.g. [37–40]). In general, previous studies assumed that different AMS evolved in response to (i) the typical surface roughness of the environment, (ii) the specific insect–plant interactions [41] or (iii) other environmental characteristics [33]. Nubby and smooth AMS are probably adaptations to the surface roughness [17,27]. Smooth ones in particular show the best performance on smooth surfaces [15], while nubby AMS operate more properly on a broad range of different levels of roughness [14–16,33].

The AMS with derived surface patterns, which split the actual contact area, such as flat pads, plateaus or mazes, are possibly adapted to wet areas, in order to reduce hydroplaning or to reduce stick-slip motions on dry surfaces [17,33]. Both effects have been demonstrated for similar artificial surfaces [42,43]. Ridges represent microstructures, which cause a

frictional anisotropy with and against their direction. The friction coefficients of such anisotropic structures differ depending on the direction the force is applied, because of the attachment pad's microsculpture [44]. This anisotropy is possibly beneficial in association with food plants that possess structured surfaces [17,27], as it potentially generates stronger grip and propulsion on such surfaces [45]. Hence, the functional principles of the AMS are only partially known from experimental biomechanical analyses. It would be helpful to investigate the specific functions of hitherto untested types and provide information about their ecological benefits. The AMS revealed no further hierarchical level of nanostructures (see electronic supplementary material, S2). The smooth attachment systems of other insects likewise lack such an additional level of nanostructures [5,6]. For example, representatives of Orthoptera [39,40], Hymenoptera [46–48], Plecoptera [49] and Blattodea [50,51] possess smooth attachment pads, sometimes with a microstructure as in the AMS of Phasmatodea, but without structures at other hierarchical levels. By contrast, fibrillar attachment devices, which consist of deformable setae [6,7,11], often include another level of hierarchical structures on these setae, as in spiders [52,53], Coleoptera [54–56] or Diptera [57–59]. In addition to the different AMS, an adhesive secretion is reported for Phasmatodea [60–65], which increases the actual contact area between the pad and the substrate [66]. Such secretions possibly ensure the sufficient attachment in this case and redress the need for additional nanostructures.

## 4.2. Evolution of attachment microstructures

The realization of certain AMS in nature is discussed to rather follow ecological circumstances and selective pressures than generally reflect phylogenetic relationships [17,27]. For example, smooth and nubby AMS are found in close correlation to certain ecological preferences. Ground-dwelling stick insects frequently possess a secondary ovipositor for oviposition into the soil [3] and exhibit nubby AMS, while the smooth AMS is more frequent in tree-dwelling species [17,27]. Derived AMS types, e.g. coarse, plateaus or mazes, are found convergently in different lineages and probably occur due to specific adaptations to the habitat of the particular species. Nevertheless, closely related species with similar ecological preferences often possess the same AMS [10,17,27]. However, many unambiguously monophyletic lineages reveal a diversity of AMS, which includes abundant independent origins of both nubby and smooth AMS [17,27]. The high flexibility in AMS development potentially benefits from demonstrated transitions between different patterns. These transitions enable rapid adaptation to environmental conditions.

## 4.3. Development of the Turing model

It is an interesting fact that as the previously studied patterns of corneal nanostructures, the AMS patterns can be also simulated using the Turing model. In contrast to the parameters used in

the previous article [20], the AMS simulation yielded another area with a lower stability but a greater variety of structures. This feature can be explained by the differences in the chemical composition and properties of the components forming the corneal nanostructures and the AMS of Phasmatodea. Among the simulated patterns, parallel ridges of small dimensions emerge as a more ordered manifestation of the maze-type structures. However, we did not observe the existence of such structures in nature, which can be explained by their lack of functionality or by insufficient sampling. Nevertheless, we were able to find two types of AMS that are related to the structures predicted by the simulation by re-evaluating the AMS in consideration of the modelled patterns. The first of these belongs to *Arabidopsis lyratus* and is a transition between the flat pad type and the predicted, but hitherto not found in nature, one (large maze-type structures, figure 2*f,k*). The second type belonging to *Eurycnema goliath* is a dimpled pattern type (figure 2*h,j*), which was initially ignored from morphological studies as a possible artefact of sample preparation. These examples illustrate the predictive power of Turing modelling.

As mentioned above, different nubby patterns occupy more area in our simulation field than any other type of pattern (figure 2), and this is the most common AMS among Phasmatodea.

## 5. Conclusion

The euplantular AMS of Phasmatodea reveals a diverse set of patterns. The formation of these patterns can be mathematically simulated by the reaction–diffusion model, revealing easy transformations between different types. As the AMS appear to be highly dependent on the ecology of the species, the ease of such transformations suggests their outstanding adaptability to the set of surface substrates in the specific habitat of the species. This indicates a high potential for the evolution of AMS during the rapid radiation of phasmatodean lineages. With a sufficiently resolved phylogeny and a broader taxon sampling, we expect a better understanding of the evolutionary pathways of phasmid AMS in the future.

**Data accessibility.** Micrographs showing a higher magnification of different AMS (electronic supplementary material, S1), the description of the types of euplantular AMS (electronic supplementary material, S2) and the taxa list (electronic supplementary material, S3) of this study are provided as the electronic supplementary material.

**Authors' contributions.** V.L.K. and S.N.G. conceived the study. T.H.B. conducted the SEM analysis. M.K. carried out the Turing modelling. T.H.B. and M.K. wrote the manuscript. V.L.K. and S.N.G. revised the manuscript. All the authors gave their final approval for publication.

**Competing interests.** We have no competing interest.

**Funding.** We received no funding for this study.

**Acknowledgements.** We thank Esther Appel and Alexander Kovalev (Department of Biomechanics and Functional Morphology, Kiel University, Kiel) for support in microscopy and specimen preparation.

## References

1. Bradler S. 2009 *Die Phylogenie der Stab- und Gespenstschrecken (Insecta: Phasmatodea)*. Göttingen, Germany: Göttingen University Press.
2. Bradler S, Cliquennois N, Buckley TR. 2015 Single origin of the Mascarene stick insects. Ancient radiation on sunken islands? *BMC Evol. Biol.* **15**, 196. (doi:10.1186/s12862-015-0478-y)
3. Buckley TR, Attanayake D, Bradler S. 2009 Extreme convergence in stick insect evolution: Phylogenetic placement of the Lord Howe Island tree lobster. *Proc. R. Soc. B* **276**, 1055–1062. (doi:10.1098/rspb.2008.1552)

4. Goldberg J, Bresseel J, Constant J, Kneubühler B, Leubner F, Michalik P, Bradler S. 2015 Extreme convergence in egg-laying strategy across insect orders. *Sci. Rep.* **5**, 7825. (doi:10.1038/srep07825)
5. Beutel RG, Gorb SN. 2001 Ultrastructure of attachment specializations of hexapods (Arthropoda): evolutionary patterns inferred from a revised ordinal phylogeny. *J. Zool. Syst. Evol. Res.* **39**, 177–207. (doi:10.1046/j.1439-0469.2001.00155.x)
6. Beutel RG, Gorb SN. 2006 A revised interpretation of the evolution of attachment structures in Hexapoda with special emphasis on Mantophasmatodea. *Arthropod Syst. Phylogeny* **64**, 3–25.
7. Beutel RG, Gorb SN. 2008 Evolutionary scenarios for unusual attachment devices of Phasmatodea and Mantophasmatodea (Insecta). *Syst. Entomol.* **33**, 501–510. (doi:10.1111/j.1365-3113.2008.00428.x)
8. Gorb SN. 2001 *Attachment devices of insect cuticle*. Dordrecht, the Netherlands: Kluwer Academic Publishers.
9. Gorb SN, Beutel RG. 2001 Evolution of locomotory attachment pads of hexapods. *Naturwissenschaften* **88**, 530–534. (doi:10.1007/s00114-001-0274-y)
10. Büscher TH, Gorb SN. 2017 Subdivision of the neotropical Prisopodinae Brunner von Wattenwyl, 1893 based on features of tarsal attachment pads (Insecta, Phasmatodea). *ZooKeys* **645**, 1–11. (doi:10.3897/zookeys.645.10783)
11. Bennemann M, Backhaus S, Scholz I, Park D, Mayer J, Baumgartner W. 2014 Determination of the Young's modulus of the epicuticle of the smooth adhesive organs of *Carausius morosus* using tensile testing. *J. Exp. Biol.* **217**, 3677–3687. (doi:10.1242/jeb.105114)
12. Arzt E, Gorb SN, Spolenak R. 2003 From micro to nano contacts in biological attachment devices. *Proc. Natl Acad. Sci. USA* **100**, 10 603–10 606. (doi:10.1073/pnas.1534701100)
13. Persson BNJ. 2013 *Sliding friction: physical principles and application*. Berlin, Germany: Springer.
14. Labonte D, Federle W. 2013 Functionally different pads on the same foot allow control of attachment: stick insects have load-sensitive 'heel' pads for friction and shear-sensitive 'toe' pads for adhesion. *PLoS ONE* **8**, e81943. (doi:10.1371/journal.pone.0081943)
15. Bußhardt P, Wolf H, Gorb SN. 2012 Adhesive and frictional properties of tarsal attachment pads in two species of stick insects (Phasmatodea) with smooth and nubby euplantulae. *Zoology* **115**, 135–141. (doi:10.1016/j.zool.2011.11.002)
16. Labonte D, Williams JA, Federle W. 2014 Surface contact and design of fibrillar 'friction pads' in stick insects (*Carausius morosus*): mechanisms for large friction coefficients and negligible adhesion. *J. R. Soc. Interface* **11**, 20140034. (doi:10.1098/rsif.2014.0034)
17. Büscher TH, Grohmann C, Bradler S, Gorb SN. 2018 Submitted. Tarsal attachment pads in Phasmatodea (Hexapoda: Insecta).
18. Richards AG, Richards PA. 1979 The cuticular protuberances of insects. *Int. J. Insect Morphol. Embryol.* **8**, 143–157. (doi:10.1016/0020-7322(79)90013-8)
19. Stavenga DG, Foletti S, Palasantzas G, Arikawa K. 2006 Light on the moth-eye corneal nipple array of butterflies. *Proc. R. Soc. B* **273**, 661–667. (doi:10.1098/rspb.2005.3369)
20. Blagodatski A, Sergeev A, Kryuchkov M, Lopatina Y, Katanaev VL. 2015 Diverse set of Turing nanopatterns coat corneae across insect lineages. *Proc. Natl Acad. Sci. USA* **112**, 10 750–10 755. (doi:10.1073/pnas.1505748112)
21. Kryuchkov M, Blagodatski A, Cherepanov V, Katanaev VL. 2017 Arthropod corneal nanocoatings: diversity, mechanisms, and functions. In *Functional surfaces in biology III. Biologically-inspired systems*, vol 10 (eds SN Gorb, EV Gorb), pp. 29–52. Cham, Switzerland: Springer.
22. Turing AM. 1952 The chemical basis of morphogenesis. *Phil. Trans. R. Soc. Lond. B* **237**, 37–72. (doi:10.1098/rstb.1952.0012)
23. Chandran R, Williams L, Hung A, Nowlin K, Lajeunesse D. 2016 SEM characterization of anatomical variation in chitin organization in insect and arthropod cuticles. *Micron* **82**, 74–85. (doi:10.1016/j.micron.2015.12.010)
24. Kryuchkov M, Lehmann J, Schaab J, Cherepanov V, Blagodatski A, Fiebig M, Katanaev VL. 2017 Alternative moth-eye nanostructures: antireflective properties and composition of dimpled corneal nanocoatings in silk-moth ancestors. *J. Nanobiotechnol.* **15**, 61. (doi:10.1186/s12951-017-0297-y)
25. Blagodatski A, Kryuchkov M, Sergeev A, Klimov AA, Shcherbakov MR, Enin GA, Katanaev VL. 2014 Under- and over-water halves of Gyrinidae beetle eyes harbor different corneal nanocoatings providing adaptation to the water and air environments. *Sci. Rep.* **4**, 6004. (doi:10.1038/srep06004)
26. Kryuchkov M, Lehmann J, Schaab J, Fiebig M, Katanaev VL. 2017 Antireflective nanocoatings for UV-sensation: the case of predatory owlfly insects. *J. Nanobiotechnol.* **15**, 52. (doi:10.1186/s12951-017-0287-0)
27. Büscher TH, Buckley TR, Grohmann C, Gorb SN, Bradler S. 2018 The evolution of tarsal adhesive microstructures in stick and leaf insects (Phasmatodea). *Front. Ecol. Evol.* **6**, 69. (doi:10.3389/fevo.2018.00069)
28. Gottardo M. 2011 A new genus and new species of Philippine stick insects (Insecta: Phasmatodea) and phylogenetic considerations. *C. R. Biol.* **334**, 555–563. (doi:10.1016/j.crvi.2011.04.003)
29. Gottardo M, Heller P. 2012 An enigmatic new stick insect from the Philippine Islands (Insecta: Phasmatodea). *C. R. Biol.* **335**, 594–601. (doi:10.1016/j.crvi.2012.07.004)
30. Gottardo M, Valotto D. 2014 External macro- and micromorphology of the male of the stick insect *Hermarchus leytensis* (Insecta: Phasmatodea) with phylogenetic considerations. *C. R. Biol.* **337**, 258–268. (doi:10.1016/j.crvi.2014.02.005)
31. Valotto D, Bresseel J, Heitzmann T, Gottardo M. 2016 A black-and-red stick insect from the Philippines—observations on the external anatomy and natural history of a new species of *Orthomeria*. *ZooKeys* **559**, 35–57. (doi:10.3897/zookeys.559.6281)
32. Gorb SN. 2008 Smooth attachment devices in insects: functional morphology and biomechanics. *Adv. Insect Physiol.* **34**, 81–115. (doi:10.1016/S0065-2806(07)34002-2)
33. Grohmann C, Henze MJ, Nørgaard T, Gorb SN. 2015 Two functional types of attachment pads on a single foot in the Namibia bush cricket *Acanthoproctus diadematus* (Orthoptera: Tettigoniidae). *Proc. R. Soc. Lond. B* **282**, 20142976. (doi:10.1098/rspb.2014.2976)
34. Gottardo M, Valotto D, Beutel RG. 2015 Giant stick insects reveal unique ontogenetic changes in biological attachment devices. *Arthropod Struct. Dev.* **44**, 195–199. (doi:10.1016/j.asd.2015.01.001)
35. Gladun D, Gumovsky A. 2006 The pretarsus in Chalcidoidea (Hymenoptera Parasitica): functional morphology and possible phylogenetic implications. *Zool. Scripta* **35**, 607–626. (doi:10.1111/j.1463-6409.2006.00245.x)
36. Schmitt M, Büscher TH, Gorb SN, Rajabi H. 2018 How does a slender tibia resist buckling? The effect of material, structural and geometric characteristics on the buckling behaviour of the hindleg tibia in the postembryonic development of the stick insect *Carausius morosus*. *J. Exp. Biol.* **221**, jeb.173047. (doi:10.1242/jeb.173047)
37. Gorb SN, Scherge M. 2000 Biological microtribology: anisotropy in frictional forces of orthopteran attachment pads reflects the ultrastructure of a highly deformable material. *Proc. R. Soc. Lond. B* **267**, 1239–1244. (doi:10.1098/rspb.2000.1133)
38. Gorb SN, Jiao Y, Scherge M. 2000 Ultrastructural architecture and mechanical properties of attachment pads in *Tettigonia viridissima* (Orthoptera Tettigoniidae). *J. Comp. Physiol. A* **186**, 821–831. (doi:10.1007/s00359000135)
39. Jiao Y, Gorb SN, Scherge M. 2000 Adhesion measured on the attachment pads of *Tettigonia viridissima* (Orthoptera, Insecta). *J. Exp. Biol.* **203**, 1887–1895.
40. Perez Goodwyn PP, Peressadko A, Schwarz H, Kastner V, Gorb SN. 2006 Material structure, stiffness, and adhesion: why attachment pads of the grasshopper (*Tettigonia viridissima*) adhere more strongly than those of the locust (*Locusta migratoria*) (Insecta: Orthoptera). *J. Comp. Physiol. A* **192**, 1233–1243. (doi:10.1007/s00359-006-0156-z)
41. Friedemann K, Kunert G, Gorb, EV, Gorb SN, Beutel RG. 2015 Attachment forces of pea aphids (*Acyrtosiphon pisum*) on different legume species. *Ecol. Entomol.* **40**, 732–740. (doi:10.1111/een.12249)
42. Varenberg M, Gorb SN. 2007 Shearing of fibrillar adhesive microstructure: friction and shear-related

- changes in pull-off force. *J. R. Soc. Interface* **4**, 721–725. (doi:10.1098/rsif.2007.0222)
43. Varenberg M, Gorb SN. 2009 Hexagonal surface micropattern for dry and wet friction. *Adv. Mater.* **21**, 483–486. (doi:10.1002/adma.200802734)
  44. Filippov A, Gorb SN. 2013 Frictional-anisotropy-based systems in biology: structural diversity and numerical model. *Sci. Rep.* **3**, 1240. (doi:10.1038/srep01240)
  45. Clemente CJ, Dirks JH, Barbero DR, Steiner U, Federle W. 2009 Friction ridges in cockroach climbing pads: anisotropy of shear stress measured on transparent, microstructured substrates. *J. Comp. Physiol. A* **195**, 805–814. (doi:10.1007/s00359-009-0457-0)
  46. Federle W, Brainerd EL, McMahon TA, Hölldobler B. 2001 Biomechanics of the movable pretarsal adhesive organ in ants and bees. *Proc. Natl Acad. Sci. USA* **98**, 6215–6220. (doi:10.1073/pnas.111139298)
  47. Federle W, Riehle M, Curtis AS, Full RJ. 2002 An integrative study of insect adhesion: mechanics and wet adhesion of pretarsal pads in ants. *Integr. Comp. Biol.* **42**, 1100–1106. (doi:10.1093/icb/42.6.1100)
  48. Frantsevich L, Gorb SN. 2004 Structure and mechanics of the tarsal chain in the hornet, *Vespa crabro* (Hymenoptera: Vespidae): implications on the attachment mechanism. *Arthropod. Struct. Dev.* **33**, 77–89. (doi:10.1016/j.asd.2003.10.003)
  49. Nelson CH. 2009 Surface ultrastructure and evolution of tarsal attachment structures in Plecoptera (Arthropoda: Hexapoda). *Aquatic Insects* **31**, 523–545. (doi:10.1080/01650420802598210)
  50. Clemente CJ, Federle W. 2008. Pushing versus pulling: division of labour between tarsal attachment pads in cockroaches. *Proc. R. Soc. B* **275**, 1329–1336. (doi:10.1098/rspb.2007.1660)
  51. Casteren A, Codd JR. 2010. Foot morphology and substrate adhesion in the Madagascan hissing cockroach, *Gromphadorhina portentosa*. *J. Insect Sci.* **10**, 1–40. (doi:10.1673/031.010.4001)
  52. Gorb SN, Niederegger S, Hayashi CY, Summers AP, Vötsch W, Walther P. 2006 Silk-like secretion from tarantula feet. *Nature* **443**, 407. (doi:10.1038/443407a)
  53. Wolff J, Gorb SN. 2012 Comparative morphology of pretarsal scopulae in eleven spider families. *Arthropod. Struct. Dev.* **41**, 419–433. (doi:10.1016/j.asd.2012.04.004)
  54. Stork NE. 1980 Experimental analysis of adhesion of *Chrysolina polita* (Chrysomelidae: Coleoptera) on a variety of surfaces. *J. Exp. Biol.* **88**, 91–108.
  55. Gorb EV, Gorb SN. 2002 Attachment ability of the beetle *Chrysolina fastuosa* on various plant surfaces. *Entomol. Exp. Appl.* **105**, 13–28. (doi:10.1046/j.1570-7458.2002.01028.x)
  56. Bullock JMR, Federle W. 2011 Beetle adhesive hairs differ in stiffness and stickiness: *in vivo* adhesion measurements on individual setae. *Naturwissenschaften* **98**, 381–387. (doi:10.1007/s00114-011-0781-4)
  57. Gorb SN. 1998 The design of the fly adhesive pad: distal tenent setae are adapted to the delivery of an adhesive secretion. *Proc. R. Soc. Lond. B* **265**, 747–752. (doi:10.1098/rspb.1998.0356)
  58. Niederegger S, Gorb SN, Jiao Y. 2002 Contact behaviour of tenent setae in attachment pads of the blowfly *Calliphora vicina* (Diptera, Calliphoridae). *J. Comp. Physiol. A* **187**, 961–970. (doi:10.1007/s00359-001-0265-7)
  59. Friedemann K, Schneeberg K, Beutel RG. 2014 Fly on the wall—attachment structures in lower Diptera. *Syst. Entomol.* **39**, 460–473. (doi:10.1111/syen.12064)
  60. Drechsler P, Federle W. 2006 Biomechanics of smooth adhesive pads in insects: influence of tarsal secretion on attachment performance. *J. Comp. Physiol. A* **192**, 1213–1222. (doi:10.1007/s00359-006-0150-5)
  61. Clemente CJ, Bullock JMR, Beale A, Federle W. 2010 Evidence for selfcleaning in fluid-based smooth and hairy adhesive systems of insects. *J. Exp. Biol.* **213**, 635–642. (doi:10.1242/jeb.038232)
  62. Dirks JH, Clemente CJ, Federle W. 2010 Insect tricks: two-phasic foot pad secretion prevents slipping. *J. R. Soc. Interface* **7**, 587–593. (doi:10.1098/rsif.2009.0308)
  63. Dirks JH, Federle W. 2011 Fluid-based adhesion in insects—principles and challenges. *Soft Matter* **7**, 11 047–11 053. (doi:10.1039/C1SM06269G)
  64. Dirks JH, Li MH, Kabla A, Federle W. 2012 *In vivo* dynamics of the internal fibrous structure in smooth adhesive pads of insects. *Acta Biomater.* **8**, 2730–2736. (doi:10.1016/j.actbio.2012.04.008)
  65. Clemente CJ, Federle W. 2012 Mechanisms of self-cleaning in fluid-based smooth adhesive pads of insects. *Bioinspir. Biomim.* **7**, 046001. (doi:10.1088/1748-3182/7/4/046001)
  66. Bullock JMR, Drechsler P, Federle W. 2008 Comparison of smooth and hairy attachment pads in insects: friction, adhesion and mechanisms for direction-dependence. *J. Exp. Biol.* **211**, 3333–3343. (doi:10.1242/jeb.020941)